Supporting information

Sensing of COVID-19 spike protein in nasopharyngeal samples using a portable surface plasmon resonance diagnostic system

Hiba Saada,[1] Quentin Pagneux,[1] James Wei,[2] Ludovic Live,[2] Alain Roussel,[3] Alexis Dogliani,[3] Lycia Die Morini,[3] Ilka Engelmann,[4] Enagnon Kazali Alidjinou,[4] Anne Sophie Rolland,[5] Emmanuel Faure,[6,7] Julien Poissy,[8] Julien Labreuche,[9] Gil Lee,[10] Peng Li,[10] Gerard Curran,[10] Anass Jawhari,[11] Jhonny A. Yunda,[12] Sorin Melinte,[12] Axel Legay,[12] Jean-Luc Gala,[13] David Devos,[5] Rabah Boukherroub,[1] Sabine Szunerits[1*]

[1]Univ. Lille, CNRS, Centrale Lille, Univ. Polytechnique Hauts-de-France, UMR 8520 - IEMN, F-59000 Lille, France

[2] Affinité Instruments, Canada

[3] Laboratoire d'Ingénierie des Systèmes Macromoléculaires (LISM), Institut de Microbiologie, Bioénergies et Biotechnologie (IM2B), Aix-Marseille Université - CNRS, UMR 7255, Marseille, France

[4] Univ Lille, CHU Lille, Laboratoire de Virologie ULR3610, F-59000 Lille, France

[5] Univ. Lille, CHU-Lille, Inserm, U1172, Lille Neuroscience & Cognition, LICEND, Lille, France

[6] Service Universitaire de maladies infectieuses - Hôpital Hutiez, CHU de Lille, F-59000, Lille, France

[7] UMR8204 U1019, Centre infection et immunité de Lille, Equipe Opinfield, Institut Pasteur de Lille, F-59800, Lille, France

[8] Univ. Lille, Inserm U1285, CHU Lille, Pôle de réanimation, CNRS, UMR 8576 - UGSF - Unité de Glycobiologie Structurale et Fonctionnelle, F-59000 Lille, France

[9] Univ. Lille, CHU Lille, ULR2694 METRICS : évaluation des technologies de santé et des pratiques médicales, F 59000 Lille, France

[10] Magnostics, 2 Clifton Lane, Monkstown, County Dublin, Ireland

[11] Biosensing Diagnostics, 310 avenue Eugène Avinée, Parc Eurasanté Ouest, 59120 Loos, France

[12] Université catholique de Louvain, ICTEAM, Louvain-la-Neuve, Belgium

[13] Université catholique de Louvain, CTMA, Brussels, Belgium

1. Experimental details

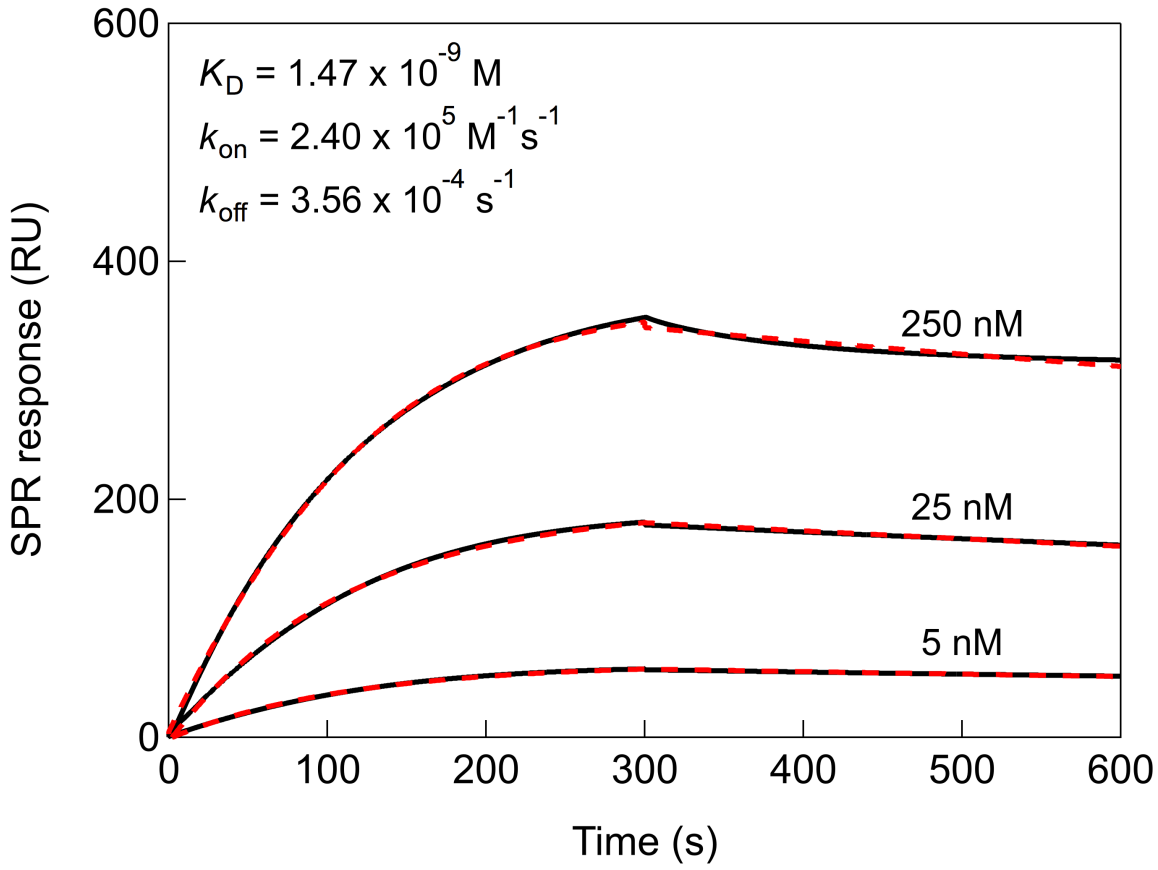

Figure S1. SPR sensorgrams measuring the apparent binding affinity of RBD Wuhan (Acrobiosystem, Ref. SPD-C52H3) to surface immobilized VHH-72-Fc (250, 25 and 5 nM) SPR chip. The SPR curves were recorded with a Biacore T200 (Cytiva Life Science) using as running buffer HBS-P+ Buffer 1× (containing 0.01 M HEPES, 0.15 M NaCl and 0.05% v/v surfactant P20). Surface modification response of 1 RU is equal to 1 pg mm^{-2} and the change of 2000 RU units was targeted with VHH-72-Fc. The interaction with RBD Wuhan was performed at a flow rate of 30 µL min^{-1}. The SPR curve is colored in black and the fit of the data to a 1:1 binding curve is colored in red.

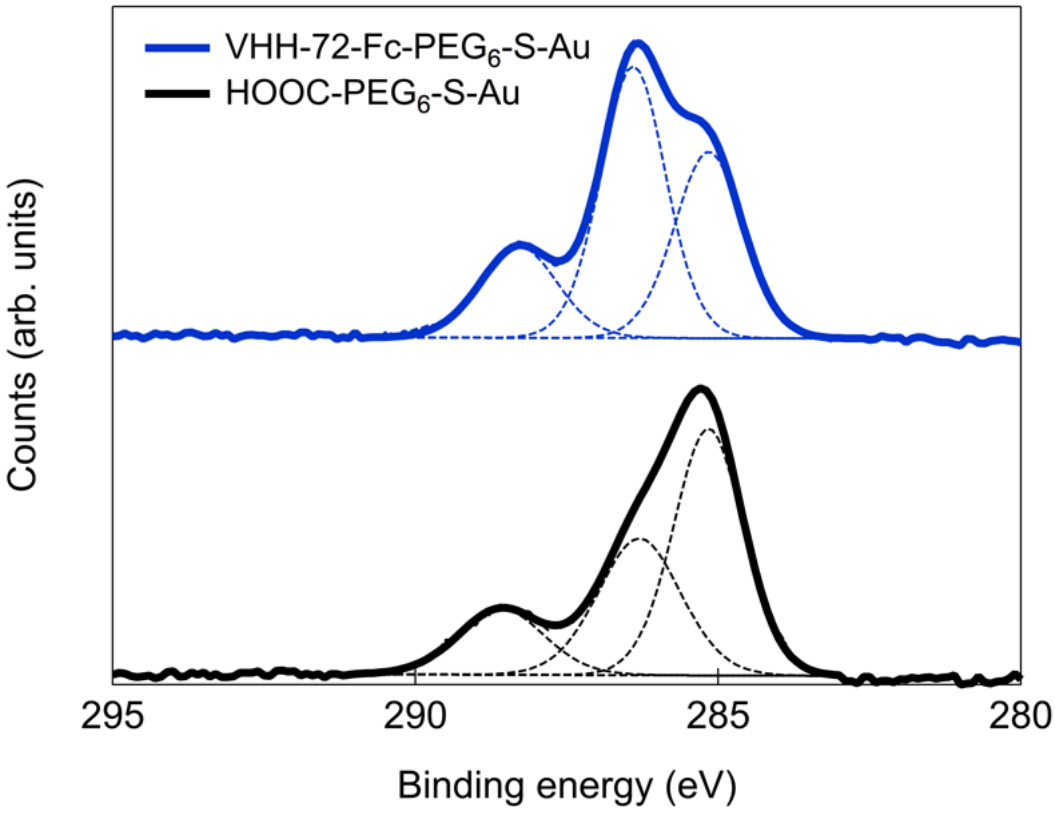

Figure S2. High resolution X-ray photoelectron spectroscopy (C_{1s} region of the spectrum) for SPR chips modified with SH-PEG_6-COOH ligand followed by covalent integration of VHH-72-Fc via amide bond.

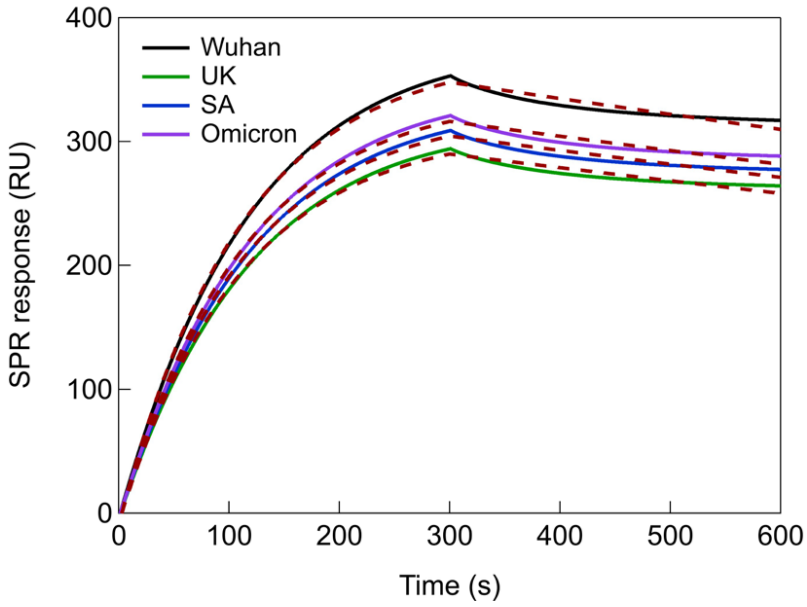

Figure S3. SPR response on VHH-72-Fc modified gold prims to different RBD mutants (100 nM): RBD Wuhan (black, Acrobiosystems, Ref. SPD-C52H3), RBD UK (green, Sinobiological, Ref. 40592-V08H8), RBD South Africa (blue, Acrobiosystems, Ref. SPD-C52H), and S1 RBD Omicron (violet, Acrobiosystems, Ref. S1N-C52Ha). The fit of the data to a 1:1 binding curve is colored in red.

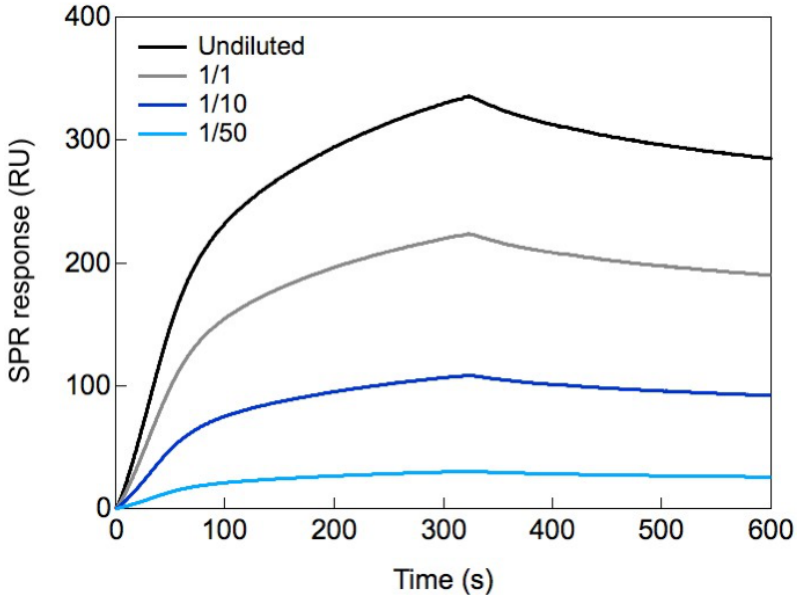

Figure S4. SPR response on VHH-72-Fc modified gold prims to undiluted negative nasopharyngeal samples (black) and negative nasopharyngeal samples diluted 1/1 (grey), 1/10 (blue) and 1/50 (bright blue) in SPR running buffer HBS-P+ Buffer 1× (containing 0.01 M HEPES, 0.15 M NaCl and 0.05% v/v surfactant P20). The interaction was performed at a flow rate of 30 µL min^{-1}.

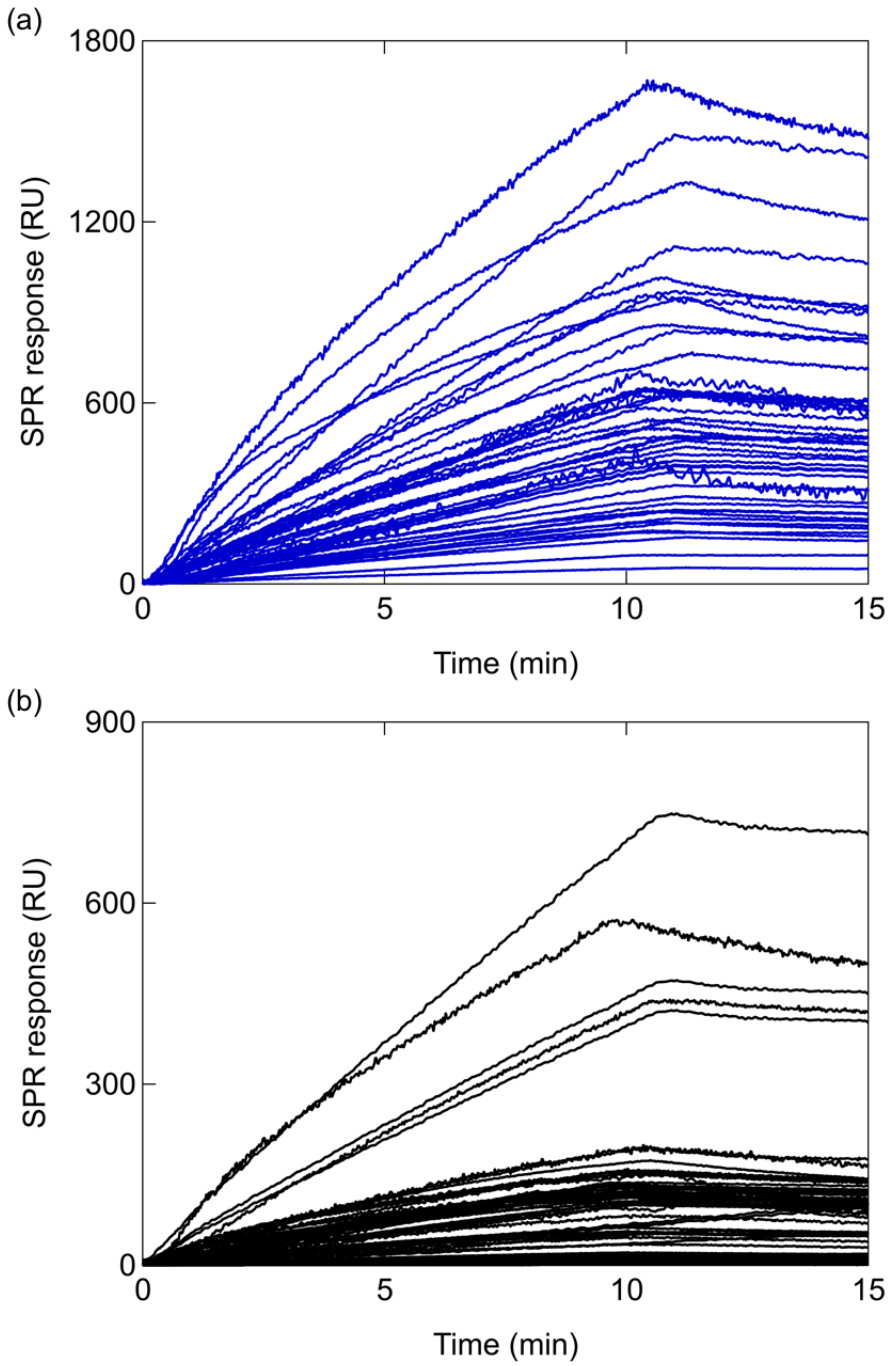

Figure S5. SPR response on VHH-72-Fc modified gold prims to 1/50 diluted clinical samples running buffer HBS-P+ Buffer 1× (containing 0.01 M HEPES, 0.15 M NaCl and 0.05% v/v surfactant P20). The interaction was performed at a flow rate of 30 µL min^{-1}. (a) RT-qPCR positive (50) nasopharyngeal samples. (b) RT-qPCR negative (69) nasopharyngeal samples.

2. Machine learning analysis

Sampling time (ms)	Sensorgram length (min) and SPR stages	Accuracy	Precision	Sensitivity	F1-Score	Specificity	Cohen's Kappa
125	15 Association and Dissociation	0.8889	0.9231	0.8000	0.8571	**0.9524**	0.7670
	5 Association	0.8889	0.8235	0.9333	0.8750	0.8571	0.7757
	1 Association	0.7778	0.6667	0.9333	0.7778	0.6667	0.5676
250	15 Association and Dissociation	0.9167	0.9286	0.8667	0.8966	**0.9524**	0.8269
	5 Association	0.9167	0.9286	0.8667	0.8966	**0.9524**	0.8269
	1 Association	**0.9722**	**0.9375**	**1.000**	**0.9677**	**0.9524**	**0.9434**
1000	15 Association and Dissociation	**0.9722**	**0.9375**	**1.000**	**0.9677**	**0.9524**	**0.9434**
	5 Association	0.9444	0.9333	0.9333	0.9333	**0.9524**	0.8857
	1 Association	0.9167	0.8333	**1.000**	0.9091	0.8571	0.8333

Table S1. Performance of machine learning models trained from sensorgrams with different sampling and acquisition times. The phases (association and dissociation) of the SPR response included for the analysed sensorgrams are indicated. The indicated metrics are calculated from the confusion matrix obtained by the execution of each model over the test database (15 positive and 21 negative).

Sensorgram length (min)	Sampling time (ms)	Response range negative (RU)	Response range positive (RU)	Cut-off value (RU)
15	125	0.81 - 308.16	234.20 - 1474.12	234 - 309
	250	0.81 - 213.86	234.12 - 1473.93	**224**
	1000	0.81 - 138.62	157.78 - 1480.35	**148**

Table S2. SPR response ranges and cut-off values obtained from the test database. The models were tested on 36 sensorgrams (15 positive and 21 negative) of the same size with three different sampling times 125, 250 and 1000 ms. Both association and dissociation stages were considered for the sensorgram length (15 min). Results are displayed in **Figure S6**.

As shown in **Table S2** and **Figure S6**, for the 1000 ms sampling time, the cut-off between positive and negative classes is 148 RU, while this value rises to 224 RU for the 250 ms sampling time. Thus, the 186 RU cut-off represents the average value obtained for the 250 and 1000 ms sampling times; this conservative value has been used in the manuscript. We note that using a cut-off of 148 RU is also fully consistent with a unique performance of the SPR device, providing a PPA of 94% (47 positive out of 50) and a NPA of 90% (62 negative out of 69).

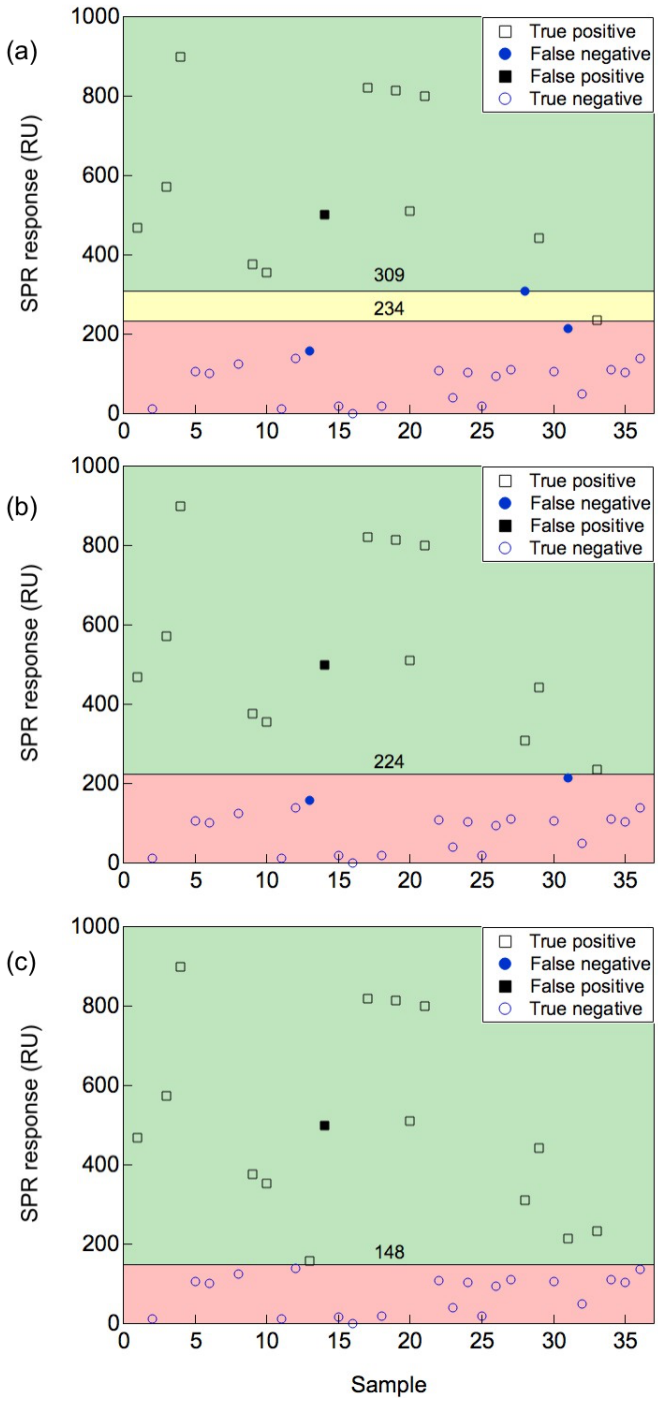

Figure S6. Determination of the positive/negative cut-off values by models trained with sensorgrams of 15 min (entire association and dissociation stages) with different sampling times ((a) – 125 ms, (b) – 250 ms, (c) – 1000 ms). The green area (with upper limit of 1000 RU for clarity) represents the zone of positive predictions and the red area represents the zone of negative predictions. The yellow area corresponds to the overlapping zone where a cut-off value for the SPR response cannot be defined.